Pleistocene Collapse of the West Antarctic Ice Sheet

Reed P. Scherer,* Ala Aldahan, Slawek Tulaczyk, Göran Possnert, Hermann Engelhardt, Barclay Kamb

Some glacial sediment samples recovered from beneath the West Antarctic ice sheet at ice stream B contain Quaternary diatoms and up to 10^8 atoms of beryllium-10 per gram. Other samples contain no Quaternary diatoms and only background levels of beryllium-10 (less than 10^6 atoms per gram). The occurrence of young diatoms and high concentrations of beryllium-10 beneath grounded ice indicates that the Ross Embayment was an open marine environment after a late Pleistocene collapse of the marine ice sheet.

The West Antarctic ice sheet (WAIS) is the world's only large ice sheet that is grounded well below sea level at its margins, making it susceptible to collapse (*1*). Collapse of the WAIS would result in a rise in eustatic sea level of 5 to 6 m. A sea level higher than at present during the penultimate interglacial [marine oxygen isotope stage 5e (MIS 5e)], 123,000 years ago (ka), has been cited as evidence of past WAIS collapse (*2*). However, it is difficult to link glacio-eustatic sea level changes of this magnitude directly to a specific glacial source. Furthermore, coeval growth or decay of different ice bodies can lead to additive or mediating effects on sea level and oxygen isotope ($\delta^{18}O$) records. Only proximal geologic data can provide clear evidence of past WAIS collapse. Here we report paleontologic and geochemical data derived from sediments recovered from beneath the WAIS that imply that open marine conditions existed in the southern part of the Ross sector of West Antarctica during the late Pleistocene, and thus that the WAIS has at least partially collapsed at least once since the late Miocene (*3*).

Collapse of the WAIS would create a seaway across parts of the West Antarctic archipelago (Fig. 1). Marine waters in the interior Ross Sea Embayment would be host to rich seasonal populations of diatoms (*4*). Cosmogenic ^{10}Be [half-life, 1.5 million years (My)] is supplied to the ocean surface through direct or indirect atmospheric fallout, and ^{10}Be atoms adhere to suspended particles in the water column (*5*). Diatoms and ^{10}Be-bearing particles accumulate on the basin floor during periods of open water, but permanent ice cover results in little or no diatom or ^{10}Be flux (*6*). Subsequent grounding generally results in erosion of the basin floor.

Fast-flowing ice stream B is underlain by a layer of deformable clay-rich diamicton, generally several meters thick. This thin blanket of sediment has been interpreted as mobile drift (till), which is actively deforming with the flow of ice and eroding underlying strata (*7*). Piston cores of unconsolidated diamicton, up to 4 m long, have been recovered through hot water–drilled access holes on ice stream B, at Upstream B (UpB) (Fig. 1) (*8*). The ice thickness is about 1030 m, the sediment surface is about 600 m below sea level, and ice flows at approximately 400 m per year.

We analyzed 19 UpB diamicton samples for diatoms (*9*) and ^{10}Be (*10*) (Table 1) [see (*11*) for site information] in search of evidence of post-Miocene marine sediment beneath the current ice sheet. We also analyzed insoluble microparticles (*12*) from four samples of glacial ice recovered from this region, within 10 m of the bed. All particles were counted, including mineral grains, volcanic glass, palynomorphs, other plant and fungal cellulose, amorphous masses, diatoms and other biogenic skeletal material, and large and small fibers. Most fibers are presumed to be laboratory contaminants. The higher the concentration of fibers, the higher the potential for contamination by diatoms and other particles.

Scherer (*3*) described a distinctive mixture of unusual diatoms in the first till sample recovered from beneath ice stream B (88-2-1-W) (*13*). The diatoms are derived from strata of differing ages and environments. The mixture of assemblages includes relatively abundant, undescribed nonmarine diatoms, which are believed to be entirely extinct and are presumed to be of upper Paleogene age (*3*). No extant nonmarine diatoms were observed. Of the marine diatoms present, more than 95% are derived from upper Miocene antarctic marine strata. Additionally, about 2% (*14*) are Quaternary marine diatoms. The neritic (meroplanktonic) diatom *Thalassiosira antarctica* dominates the Quaternary assemblage. This diatom has an age of less than 0.75 My (*15*). The dominance of upper Miocene diatoms supports the view that West Antarctica entered a dominantly glacial phase near the end of the Miocene (*16*).

Till recovered by piston coring and other methods, from about 1 km grid west of sample 88-2-1-W toward the center of the ice stream (boreholes 89-2 and 91-2), contain rare upper Miocene diatoms but no Quaternary marine, Quaternary nonmarine, or extinct nonmarine diatoms. Samples that represent the uppermost sediments (Table 1), which are in closest proximity with the ice,

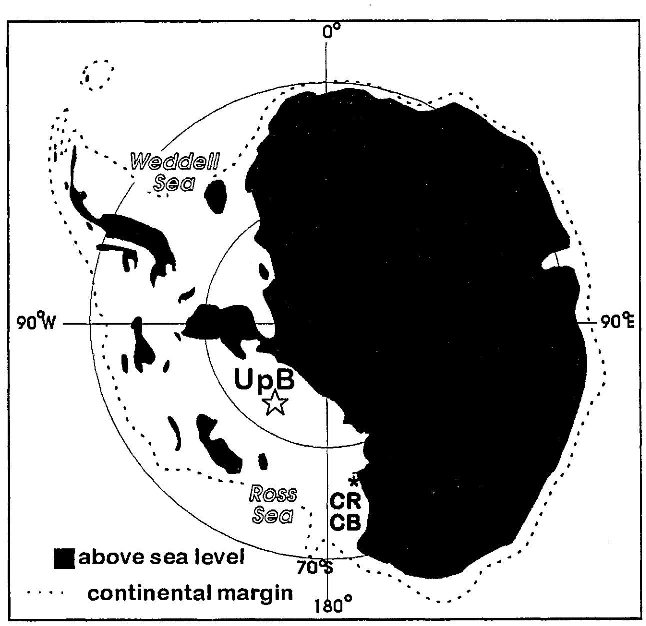

Fig. 1. Approximate configuration of West Antarctic seaways after the complete collapse of the WAIS. The setting would include some combination of open water, sea ice, fringing ice shelves, coastal tidewater glaciation, and ice tongues. Transantarctic surface water circulation would be limited by crustal geometry and ice distribution. The locations of UpB, Cape Roberts (CR), and Cape Barne (CB) are indicated.

R. P. Scherer and A. Aldahan, Department of Earth Sciences, Uppsala University, Villavägen 16, S-752 36 Uppsala, Sweden. S. Tulaczyk, H. Engelhardt, B. Kamb, Department of Geological and Planetary Sciences, California Institute of Technology, Mail Code 170-25, Pasadena, CA 91125, USA. G. Possnert, Tandem Laboratory, Ångström Laboratory, Box 533, Uppsala University, Uppsala, Sweden.

*To whom correspondence should be addressed. E-mail: reed.scherer@natgeog.uu.se

contain a relatively higher abundance of diatom fragments but no evidence that the till includes a Quaternary marine component. Similar results were obtained from core 95-1-1, recovered approximately 8 km (*17*) directly upstream of boreholes 89-2 and 91-2.

Boreholes 95-3, 95-5, 95-6, and 95-8 were drilled along a transect 1 km grid east of borehole 95-1 (*11*) in a region approximately 7 km (*17*) directly upstream of sample 88-2-1-W. Seismic properties in this region suggest that the deformable till layer is unusually thin or is entirely absent (*18*). Four diamicton samples from this region contain a high concentration of diatom fragments (Table 1 and Fig. 2) and a mixture of diatoms that is strikingly similar to that in sample 88-2-1-W: Diverse and well-preserved Quaternary marine taxa are present among a suite of dominant upper Miocene diatoms. The Quaternary diatoms include many small varieties not encountered in winnowed sample 88-2-1-W (*3*). The assemblage contains *T. antarctica* (*15*) along with diatoms *Fragilariopsis curta*, *F. kerguelensis*, *F. angulata*, *F. separanda*, *F. ritscherii*, *T. lentiginosa*, *T. tumida*, *T. gracilis*, *T. gracilis* var. *expecta*, *Actinocyclus actinochilus*, and other diatoms characteristic of Quaternary antarctic continental shelf sediments. Lower Pleistocene diatoms characteristic of the antarctic continental shelf, such as *A. ingens* and *T. elliptopora*, are not present nor are mid-Pliocene continental shelf diatoms. The above assemblage implies that the till is derived in part from sediment deposited within the past 0.75 My (*15*) and probably within the past 600 ka (*3*). These samples also contain rare examples of the unusual, extinct nonmarine diatoms present in sample 88-2-1-W. As with all other tills from ice stream B studied, no extant antarctic lacustrine diatoms were found.

These four diatom-rich, Quaternary diatom–bearing till samples also contain a significant concentration of ^{10}Be (10^8 atoms/g), whereas the remainder of the till samples, which contain no Quaternary diatoms, have only background levels of ^{10}Be ($<10^6$ atoms/g) (Table 1 and Fig. 2). A ^{10}Be concentration of 10^8 atoms/g in a typical marine sediment suggests a maximum age of 3 My (*5*, *6*). However, sediment mixing and dilution with older sediments would imply that some components of the till are younger. Dilution is demonstrated by the observation that most of the diatoms in these diamictons are Miocene in age. The absence of ^{10}Be in the remaining 11 diamicton samples analyzed suggests that the till is derived from Miocene or older rocks, with little or no incorporation of Pliocene or Quaternary marine sediment. This result is in agreement with the diatom data. The lack of ^{10}Be in these 11 samples, including samples near the ice contact zone (Table 2), indicates that melting basal ice is an in-

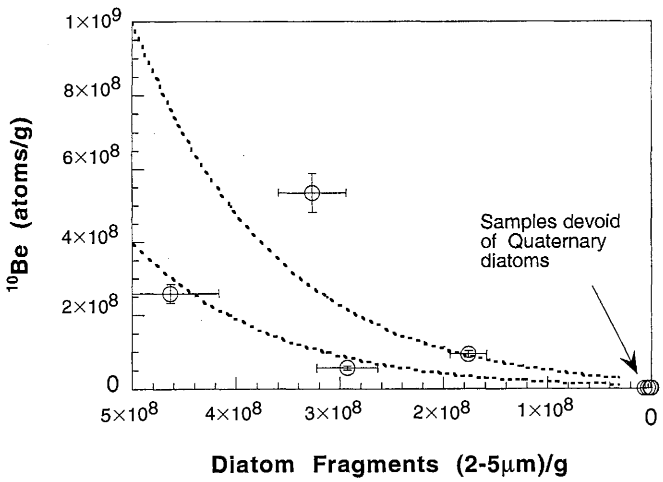

Fig. 2. ^{10}Be of UpB diamictons plotted against the total content of diatom fragments. Theoretical decay curves of ^{10}Be (half-life = 1.5 My, plotted for five half-lives) starting at 10^9 and 10^4 atoms/g [average maximum and minimum values of modern marine sediments (*5*, *6*)]. The four samples showing elevated ^{10}Be have components representing an age range of 0 to 3 My, depending on their initial ^{10}Be value. Samples containing high ^{10}Be also contain high diatom abundance.

Table 1. UpB diatom fragment abundance and ^{10}Be concentration. Samples are from piston cores unless otherwise indicated. Samples containing high ^{10}Be also contain Quaternary diatoms and extinct nonmarine diatoms.

Sample	Diatom fragments per g	^{10}Be atoms per g
88-2-1-W*	3.03×10^6	–*
95-3-1, 3–8 cm	3.27×10^8	$(5.35 \pm 0.25) \times 10^8$
95-5-1, 3–8 cm	2.93×10^8	$(5.64 \pm 0.32) \times 10^7$
95-6-4, 3–8 cm	4.63×10^8	$(2.59 \pm 0.61) \times 10^8$
95-8-1, 3–8 cm	1.76×10^8	$(9.38 \pm 0.30) \times 10^7$
95-5-3, 15–22 cm†	8.72×10^5	$<10^6$
89-2, 3–8 cm	5.44×10^5	$<10^6$
89-2, 22–28 cm	4.26×10^5	$<10^6$
91-2-3-BT‡	8.66×10^6	$<10^6$
91-2-5-BT‡	6.55×10^6	$<10^6$
95-1-1-CW§	5.10×10^6	–§
95-1-1, 5–8 cm	8.05×10^5	$<10^6$
95-1-1, 32–38 cm	3.58×10^5	–
95-1-1, 72–78 cm	2.10×10^5	$<10^6$
95-1-1, 96–100 cm	2.43×10^5	$<10^6$
95-1-1, 112–117 cm	3.84×10^5	$<10^6$
95-1-1, 186–191 cm	6.34×10^5	$<10^6$
95-1-1, 122–128 cm	8.23×10^5	$<10^6$
95-1-1, 296–300 cm	2.77×10^5	–

*Sample winnowed in recovery, biasing diatom abundance. Not appropriate for Be analysis. †Third core from borehole 95-5. Sediment recovered represents till stratigraphically below core 95-5-1. Exact depth not known (~1 to 4 m). ‡BT: Borehole toll inserted into till, recovered from near the sediment surface. §CW: Core water (sediment suspended above recovered core). Insufficient sediment was available in the CW sample for ^{10}Be analysis.

Table 2. Particles in UpB ice, less than 10 m above sediment surface.

Ice sample	95-8-1-2	95-8-1-5	95-2-6-1	95-2-3-2
Sample volume (ml)	218	235	149	173
Whole marine diatoms* (*n*)	1	1	0	0
Marine diatom fragments† (*n*)	1	2	1	1
Whole nonmarine diatoms (*n*)	2	3	5	0
Nonmarine diatom fragments† (*n*)	2	3	0	0
Unidentifiable diatom fragments‡ (*n*)	4	17	9	4
Chrysophyte cysts (*n*)	3	0	0	1
Pollen/spores/fungal spores (*n*)	3/5/2	2/4/2	0/2/3	3/5/11
Mineral and volcanic grains (>5 μm) (*n*)	147	177	70	72
Fibers§ (*n*)	124	9	10	62

*Largest diatom is 12 μm. †Possible identification to genus level. See text. ‡All diatom fragments are <5 μm. §Presumed laboratory contaminants.

significant source of ^{10}Be to the subglacial sedimentary environment. To attain ^{10}Be concentrations as high as 10^8 atoms/g strictly through basal melting would require continuous accumulation of ^{10}Be in the bed for tens of thousands of years, which is unlikely beneath a flowing ice stream because of glacial erosion and an active and variable basal hydrologic system.

The diatom concentration in ice samples from near the bed of boreholes 95-2 and 95-8 ranges from 6 to 34 diatoms/liter (Table 2). Most identifiable diatoms are extant nonmarine forms, all of which are common to antarctic coastal lakes and lake deposits. Only two identifiable marine diatoms were found on the filters: one small (13 μm) specimen of a recrystallized *Paralia sulcata* (sample 95-8-1-5), which is almost certainly derived from Miocene or older deposits, and one small (6 μm) *Chaetoceros* resting spore valve (sample 95-8-1-2) (*19*). The only other evidence of marine diatom debris includes rare fragments (<4 μm) of *Thalassiothrix* or *Thalassionema* and unidentifiable marine centric diatom "meshwork." Of the identifiable nonmarine diatoms, 60% are *Luticola* spp., a cosmopolitan nonmarine diatom occurring in virtually all antarctic coastal lakes and moist soils. This diatom is a common, often dominant, component of dry lake sediments in Antarctica.

Variability in diatom assemblages and ^{10}Be levels demonstrates that the basal sedimentary facies beneath ice stream B are complex. Till samples that contain these tracers provide evidence that marine conditions prevailed deep within the West Antarctic interior at some times during the Quaternary. Samples lacking such evidence imply that different source beds lie beneath the till layer or upstream. There is no evidence to suggest that the Quaternary tracers, which include diatoms as large as 65 μm, were introduced to the subglacial environment by atmospheric fallout onto the ice sheet surface and subsequent subglacial melting. Extant nonmarine diatoms are by far the most abundant diatoms in filtered glacial ice from Antarctica (*20*), including ice directly overlying sediments containing Quaternary marine diatoms (Table 2). If the age-diagnostic Quaternary marine diatoms beneath the WAIS were emplaced by release of englacial debris by basal melting, then they would be outnumbered by extant nonmarine diatoms such as *Luticola* spp. No extant nonmarine diatoms have been observed in UpB subglacial sediments.

Glaciological models suggest that it is unlikely that grounded ice could be sustained over the deep interior basins, which reach depths of more than 2000 m, given open water as far south as UpB (*1*). Therefore, we interpret the occurrences of Quaternary-age diatoms and significant concentrations of ^{10}Be in sediments beneath the WAIS as direct evidence of marine deposition in the West Antarctic interior after one or more partial (Ross Sector) or complete marine ice sheet collapse events during the past 0.75 My. These data provide no information regarding Pliocene or early Pleistocene deglacials. Evidence of such events has probably been removed from the inner Ross Embayment by glacial advances (*21*).

The Southern Ocean was warmer than at present during certain late Quaternary intervals. Most notable of these warm periods, and the most likely candidate for the time of WAIS collapse, is MIS 11, 400 ka (*3*). This interglacial was of unusually long duration and was characterized by biogenic carbonate deposition in the high-latitude Southern Ocean and unusually deep southerly penetration of North Atlantic deep water (*22*). WAIS retreat during one or more earlier or subsequent interglacials, including MIS 5e, or collapse out of phase with the climate cycle (*23*) cannot be ruled out. Given the remaining uncertainties regarding ice sheet mechanics and climatic forcing, it is not yet possible to predict the probability of WAIS collapse within the coming centuries, but geologic evidence of past collapse and observations of rapid ongoing changes in the WAIS (*1*, *24*) underscore the need for continued study.

References and Notes

1. R. B. Alley and I. M. Whillians, *Science* **254**, 959 (1991); D. R. MacAyeal, *Nature* **359**, 29 (1992); C. R. Bentley, *Science* **275**, 1077 (1997); R. Bindschadler, *ibid.* **276**, 5313 (1997); R. A. Warrick *et al.*, in *Second Assessment Report of the Intergovernmental Panel on Climate Change: Working Group I*, J. T. Houghton *et al.*, Eds. (Cambridge Univ. Press, Cambridge, 1996).
2. J. H. Mercer, *Nature* **271**, 321 (1978). The exact elevation of sea level during peak MIS 5e is still somewhat unclear. Recent well-dated records indicate a complex sea level history for MIS 5e, characterized by typical elevations of 2 m and at least one relatively brief eustatic high stand of at least 6 m [A. C. Neuman and P. J. Hearty, *Geology* **24**, 775 (1996); P. Kindler and A. Strasser, *ibid.* **25**, 1147 (1997); C. E. Sherman *et al.*, *ibid.* **21**, 1079 (1993)].
3. R. P. Scherer, *Palaeogeogr. Palaeoclimatol. Palaeoecol.* **90**, 359 (1991); *J. Glaciol.* **39**, 716 (1993); L. H. Burckle, *ibid.*, p. 491.
4. D. M. Harwood, R. P. Scherer, P.-N. Webb, *Mar. Micropaleontol.* **15**, 91 (1989); R. P. Scherer, thesis, Ohio State University, Columbus, OH (1992).
5. A. Eisenhauer *et al.*, *Earth Planet. Sci. Let.* **124**, 171 (1994); C. F. You *et al.*, *Geochim. Cosmochim. Acta* **58**, 4887 (1994); R. F. Speilhagen *et al.*, *Geology* **25**, 783 (1997); A. Aldahan, S. Ning, G. Possnert, J. Backman, K. Boström, *Mar. Geol.* **144**, 147 (1997).
6. A. Aldahan and G. Possnert, *Quat. Sci. Rev.*, in press.
7. R. B. Alley, D. D. Blankenship, C. R. Bentley, S. T. Rooney, *Nature* **322**, 57 (1986); D. D. Blankenship, C. R. Bentley, S. T. Rooney, R. B. Alley, *ibid.*, p. 54; H. Engelhardt, N. Humphrey, B. Kamb, M. Fahnstock, *Science* **248**, 57 (1990).
8. S. Tulaczyk, B. Kamb, R. P. Scherer, H. Engelhardt, *J. Sediment. Res.* **68**, 487 (1998).
9. We estimated the absolute abundance of diatoms using a modification of a recognized method [R. P. Scherer, *J. Paleolimnol.* **12**, 171 (1994)]. Abundance is normally estimated on the basis of whole diatoms, with the use of standardized counting criteria, but whole diatoms are too rare in these sediments to allow statistically significant estimates. Instead, we counted diatom fragments in the size class from 2 to 5 μm (Table 1). The abundance of whole diatom valves is at least three orders of magnitude lower. Extracting identifiable diatoms from these diamictons for biostratigraphic application requires specialized laboratory methods and extreme care to avoid sample contamination. All glassware and reusable supplies used in sample preparation are soaked in warm 15% NaOH for 4 hours and repeatedly rinsed with distilled and filtered water to remove any diatom residues that may be present. To test the reproducibility of abundance estimates and to test for potential laboratory contamination, we routinely prepare and analyze both sample duplicates and blanks. Duplicate preparations demonstrated consistent and reproducible results in diatom abundance (<10% error) and assemblage analyses. Thorough analysis of blanks revealed no evidence of sample contamination by identifiable diatom fragments.
10. AMS analysis of ^{10}Be was performed at the Uppsala Tandem Laboratory with a machine and statistical error of 5% because of boron correction and correction for the NIST SRM 4325 standard. ^{10}Be was extracted from 0.5 to 1 g of a dried silt-clay fraction, using 200 μg of Be carrier, total dissolution (with hydrochloric acid and hydrofluoric acid), and cation column separation. ^{10}Be (measured in atoms per gram) was normalized for the total sample dried at 110°C for 6 hours. The silt-clay fraction used is dominated by quartz, with lesser quantities of feldspar and clay minerals and negligible carbonate (*8*).
11. H. Engelhardt and B. Kamb, *J. Glaciol.* **43**, 207 (1997).
12. Ice samples [M. Jackson and B. Kamb, *J. Glaciol.* **43**, 415 (1998)] were washed under a stream of distilled deionized water to remove approximately 0.5 cm of the outer layers, then melted in new nylon beakers and filtered onto 25-mm microfilters. Additionally, two water blanks were filtered and analyzed (*9*). Filters were mounted on cover glass with Norland optical adhesive and analyzed in their entirety at ×1200 magnification. The age of the ice samples is unknown but is likely to be early Holocene.
13. This sample was taken during field season 1988–1989 (borehole 2, sample 1, Winnower sample). Much of the clay and other fine-grained material was lost in recovery of this sample (*3*).
14. This percentage is an underestimate because it does not include the many extant antarctic diatoms that were also common in the Miocene ocean.
15. Although it is ubiquitous in modern antarctic continental shelf sediments, the age of the first stratigraphic occurrence of *T. antarctica* is not yet well documented because of a lack of continuous Quaternary near-shore reference sections. Its appearance can be reliably bracketed by its occurrence in MIS 5e interglacial deposits [B. L. Ward and P.-N. Webb, *J. Foram. Res.* **16**, 176 (1986)] at Cape Barne, Ross Island [R. P. Scherer, unpublished data] and by its absence from well-dated (0.75 My) lower Quaternary diatomaceous deposits in the Southern Ocean [R. Gersonde and M. Barcena, *Micropaleontology* **44**, 84 (1998)] and in McMurdo Sound (Fig. 1) (Cape Roberts Project core 1, unit 3.1, upper *A. ingens* zone) [Cape Roberts Science Team, *Terra Antarctica* **5**, 1 (1998)]. J. Barron [*U.S. Geol. Surv. Open File Report* **96-173** (1996)] reports *T.* cf. *antarctica* in mid-Pliocene Antarctic sediments, but we believe that there are significant taxonomic differences between *T.* cf. *antarctica* sensu Barron and *T. antarctica* sensu stricto, which occurs in our samples.
16. G. Brancolini, A. K. Cooper, F. Coren, in *Geology and Seismic Stratigraphy of the Antarctic Margin*, A. K. Cooper, P. F. Barker, G. Brancolini, Eds., vol. 68 of *Antarctic Research Series* (American Geophysical Union, Washington, DC, 1995), p. 209; D. E. Hayes and L. A. Frakes, *Init. Repts. Deep Sea Drill. Proj.* **28**, 912 (1975).
17. The distance is reported with respect to the bed, compensated for ice stream flow between 1988 and 1995.
18. S. T. Rooney, D. D. Blankenship, R. B. Alley, C. R. Bentley, *J. Geophys. Res.* **92**, 8913 (1987).
19. The *Chaetoceros* spore occurs in the sample containing the highest concentration of clothing fibers, thus the highest potential for sample contamination.

20. D. E. Kellogg and T. B. Kellogg, *Geology* **24**, 115 (1996).
21. A massive volume of Pliocene and Pleistocene sediment has been eroded and transported toward the continental shelf edge by glacial processes [A. K. Cooper *et al.*, *Mar. Geol.* **102**, 175 (1991); R. P. Scherer, *Antarct. J. U.S.* **29**, 11 (1994)] (*16*).
22. W. R. Howard, *Nature* **388**, 418 (1997); D. A. Hodell, *Paleoceanogr.* **8**, 47 (1993).
23. D. R. MacAyeal, *Nature* **359**, 29 (1992).
24. R. Bindschadler and P. Vornberger, *Science* **279**, 689 (1998); C. S. M. Doake, H. F. J. Corr, H. Rott, P. Skvarca, N. W. Young, *Nature* **391**, 778 (1998); H. Rott, P. Skvarca, T. Nagler, *Science* **271**, 788 (1996).
25. Support for this study came from Uppsala University, the Swedish Natural Sciences Research Council, and the Knut and Alice Wallenberg Foundation to R.P.S., A.A., and G.P., and from a U.S. NSF grant OPP9319018 to B.K. and H.E.

14 April 1998; accepted 14 May 1998

Effects of Water on the α-β Transformation Kinetics in San Carlos Olivine

Tomoaki Kubo,* Eiji Ohtani, Takumi Kato, Toru Shinmei, Kiyoshi Fujino

In experiments at 13.5 gigapascals and 1030°C, the growth rate of wadsleyite, which forms from transformation of olivine, was substantially enhanced by the presence of water. Wadsleyite had a low dislocation density and subgrain boundaries in wet runs. Water enhanced the dislocation recovery in wadsleyite and therefore caused inelastic relaxation of the localized pressure drop associated with the transformation, resulting in an increase of the growth rate in wet runs. These results imply that even a small amount of water of 0.05 weight percent can weaken wadsleyite in the mantle.

Water enhances the creep of many minerals, a process termed hydrolytic weakening or water weakening (*1*). To understand the dynamics of the mantle transition zone, it is important to know the effect of water on the plastic deformation of wadsleyite, a high-pressure polymorph of olivine and a major constituent in the mantle transition zone. Wadsleyite can contain a substantial amount of H_2O, up to about 3 weight % (*2*). Chen *et al.* (*3*) analyzed broadening of powder x-ray diffraction lines and suggested that water had little effect on deformation of wadsleyite up to 10 GPa at low temperature of ~600°C. Here we present evidence that water weakens wadsleyite, by examining transformation kinetics of olivine in wet and dry conditions.

We carried out high-pressure experiments using a 3000-ton multianvil (MA) press (*4*). The experiments were performed at 13.5 GPa and 1030°C, which is within the stability field of wadsleyite (*5*). Runs lasted from 0 to 1200 min. The starting material was single crystals of San Carlos olivine $(Mg_{0.89}Fe_{0.11})_2SiO_4$ that we cut into 1-mm^3 cubes. We used a stepped graphite heater, in which the central part is thicker than upper and lower parts. A sample was encased in a fine powder of NaCl in the central part of the heater in the dry runs. In the wet runs, the olivine was enclosed by a 10:1 or 500:1 mixture of NaCl and $Mg(OH)_2$ brucite by weight. We used a sealed platinum capsule in one of the wet runs. Temperature was measured between upper and center parts of heater with a Pt-Pt13%Rh thermocouple (*6*). Samples were first compressed at room temperature and then heated to the desired value. The heating rate, which was controlled to be same in all of experiments, was about 100°C per min. The sample was quenched to room temperature at high pressure, and then the pressure was released slowly over a period of several hours.

In the recovered samples, we observed a sharply defined rim of the product phase in both dry and wet [NaCl:$Mg(OH)_2$ = 500:1] runs (Fig. 1). X-ray diffraction analysis indicated that this phase was wadsleyite. Transmission electron microscope (TEM) observations (*7*) showed that the newly grown wadsleyite rim had no topotactic relations with the host olivine. This observation suggests that the wadsleyite nucleated randomly on the olivine surface. The only apparent compositional differences, on the basis of electron microprobe analysis, between relict olivine and the reaction rim was that the rims had a few tiny iron-rich grains (*8*). Thus, we conclude that the olivine transformed to wadsleyite by incoherent surface nucleation and interface-controlled growth. This result is consistent with previous studies with mantle olivine (*9*).

In the dry runs, wadsleyite growth was retarded with time and eventually ceased after 200 min (Fig. 2). In contrast, in the wet [NaCl:$Mg(OH)_2$ = 500:1] runs, the wadsleyite grew more rapidly than in the dry run, resulting in the large difference in the growth distance between the dry and wet conditions. When the ratio of NaCl and $Mg(OH)_2$ was 10:1, the transformation was completed within 180 min. These observations imply that the growth rate of the wadsleyite rim was enhanced by the presence of water in the

Fig. 1. Optical photomicrograph under crossed nichols of a thin section of an olivine single crystal partially transformed to wadsleyite at 13.5 GPa and 1030°C for 1200 min. The sample was enclosed by a mixture of NaCl and $Mg(OH)_2$ with a ratio of 500:1 by weight. The relict olivine is surrounded by the reaction rim consisted of elongated β-phase grains. Bar, 0.5 mm.

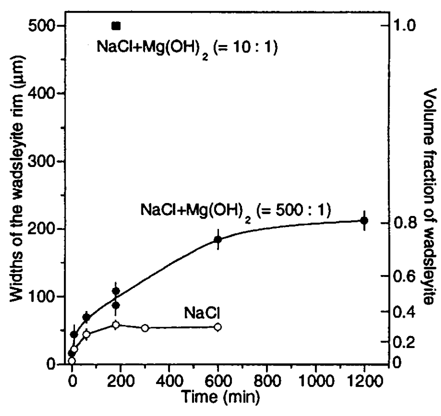

Fig. 2. Time dependence of the width and volume fraction of the wadsleyite rim in dry and wet runs at 13.5 GPa and 1030°C. The confining medium of the sample is also shown. The volume fraction of wadsleyite was estimated from widths of the wadsleyite rim. Time indicates the heating duration at the desired temperature.

T. Kubo and E. Ohtani, Institute of Mineralogy, Petrology, and Economic Geology, Faculty of Science, Tohoku University, Sendai 980–8578, Japan. T. Kato, Institute of Geoscience, University of Tsukuba, Tsukuba 305–0006, Japan. T. Shinmei and K. Fujino, Division of Earth and Planetary Sciences, Graduate School of Science, Hokkaido University, Sapporo 060–0810, Japan.

*To whom correspondence should be addressed.